

On re-brightening afterglows of XRFs, Soft GRBs and GRB081028

Shlomo Dado¹ and Arnon Dar²

ABSTRACT

It has been claimed recently that Swift has captured for the first time a late-time afterglow re-brightening of clear nonflaring origin after the steep decay of the prompt emission in a long gamma-ray burst (GRB), which may have been produced by a narrow jet viewed far off-axis. However, this interpretation of the observed re-brightening of the X-ray afterglow (AG) of GRB081028 is unlikely in view of its large equivalent isotropic gamma-ray energy. Moreover, we show that the late-time re-brightening of the AG of GRB081028 is well explained by the cannonball (CB) model of GRBs as a synchrotron flare emitted when the jet that produced the GRB in a star formation region (SFR) in the host galaxy crossed the SFR boundary into the interstellar medium or the halo of the host galaxy. We also show that all the other observed properties of GRB081028 and its afterglow are well reproduced by the CB model. On the other hand, we demonstrate that far-off axis GRBs, which in the CB model are ‘soft’ GRBs and XRFs and consequently have much smaller isotropic equivalent gamma-ray energies, have slowly rising afterglows with a late-time power-law decay identical to that of ordinary GRBs, in good agreement with the CB model predictions.

Subject headings: gamma rays: bursts

1. Introduction

A smoothly rising X-ray afterglow (AG) following the steep decay of the prompt emission in a long gamma ray burst (GRB) was first observed in GRB970508 with the Narrow Field Instrument (NFI) aboard the BeppoSAX satellite (Piro et al. 1998). Contemporaneous

¹dado@phep3.technion.ac.il

Physics Department, Technion, Haifa 32000, Israel

²arnon@physics.technion.ac.il

Physics Department, Technion, Haifa 32000, Israel

optical observations with ground based telescopes detected a corresponding re-brightening of its optical afterglow beginning around 6×10^4 sec after burst (e.g., Galama et al. 1998 and references therein). This re-brightening was interpreted by Piro et al. (1998) as due to a delayed activity of the central GRB engine. Chiang & Dermer (1997) and Dar & De Rújula (2000) showed that a rise in the afterglow of a GRB produced by a jet of highly relativistic plasmoids (Shaviv & Dar 1995) can result also from its deceleration if its viewing angle was initially far outside its relativistic beaming cone (far off-axis viewing angle). Both interpretations, however, failed to reproduce well enough the lightcurve of the AG of GRB970508. Consequently, Dado, Dar & De Rújula (hereafter DDD) 2002 have investigated alternative explanations and showed that the late-time re-brightening of the AG of GRB970508 could be explained by the encounter of the jet with a density bump such as that expected at the boundary of the star formation region (SFR) where the GRB took place. A similar re-brightening of the X-ray afterglow of GRBs was later observed with the Swift X-ray telescope (XRT) in a few GRBs, e.g., in GRB060614 (Mangano et al. 2007) and in several other GRBs where gaps in the data sampling and low statistics prevented a firm conclusion (e.g., GRBs 051016B and 070306, Swift lightcurve repository, Evans et al. 2007,2009).

Overlooking the above, Margutti et al. (2009) have recently claimed that Swift has captured for the first time a smoothly rising X-ray re-brightening of clear non-flaring origin after the steep decay of the prompt emission in a long gamma-ray burst GRB081028, which may have been produced by a narrow jet viewed far off-axis. But, the ‘far off-axis viewing’ of GRB081028 is not supported by its large equivalent isotropic gamma-ray energy: The radiation emitted by a highly relativistic jet with a bulk motion Lorentz factor $\gamma \gg 1$, which is observed from a small angle ($\theta \ll 1$) relative to its motion, is amplified by a factor δ^3 resulting from relativistic beaming and Doppler boosting, where the Doppler factor δ is well approximated by $\delta(t) = [\gamma(t) (1 - \beta(t) \cos\theta)]^{-1} \approx 2\gamma / (1 + \gamma^2 \theta^2)$ (e.g. Shaviv & Dar 1995; Dar 1998). Hence, for the typical viewing angle of GRBs, $\theta \sim 1/\gamma$, $\delta \sim \gamma$, and the observed GRB fluence is amplified by a factor γ^3 relative to that in the jet rest frame. For ‘far off-axis viewing’ angles where $\gamma^2 \theta^2 \gg 1$, this amplification of E_{iso} is reduced by a factor $[(1 + \gamma^2 \theta^2)/2]^{-3}$. For example, for $\theta = 3/\gamma$, E_{iso} is reduced by a factor 8×10^{-3} and GRBs viewed at $\theta \geq 3/\gamma$ appear as X-ray flashes (XRFs) rather than ordinary GRBs (see, e.g., Dar & De Rújula 2000; DDD2004). From the observations of GRB081028, with the Burst Alert Telescope (BAT) aboard Swift, Margutti et al. (2009) inferred that $E_{iso} = (1.1 \pm 0.1) \times 10^{53}$ erg, which is typical of ordinary GRBs and is inconsistent with the far off-axis interpretation of the re-brightening of its AG.

Despite the many serious discrepancies between the observed properties of GRB081028 and the predictions of the fireball (FB) model, which were pointed out by Margutti et al. (2009) and are quite common in many other GRBs, alternative models of GRBs were

ignored in their paper. One such model is the cannonball (CB) model, which has been shown repeatedly to reproduce well the main observed properties of GRBs and their AGs (DDD2009a and references therein). Thus, in this paper, we demonstrate that the main observed properties of GRB081028 and its afterglow are well reproduced by the CB model of GRBs. In particular, we show that the observed late-time re-brightening of the AG of GRB081028 is well explained as being a late-time synchrotron radiation (SR) flare. Such flares are expected to be emitted by the jet which produced the GRB, when it crosses the boundary of the star formation region, where presumably the GRB took place, into the ISM or the halo of the host galaxy. Moreover, we show that GRBs which have much larger viewing angles than those of ordinary GRBs, and thus appear as X-ray flashes (XRFs) or ‘soft’ GRBs, have rather slowly rising late-time afterglows which are well described by the CB model.

2. ICS and SR flares in the CB model

2.1. ICS flares

The many similarities between the prompt emission pulses in gamma ray bursts (GRBs) and X-ray flares during the fast decay phase of the prompt emission and the early afterglow suggest a common origin. In the CB model of long GRBs this common origin is bipolar ejection of highly relativistic plasmoids (CBs) following mass accretion episodes of fall-back matter on the newly born neutron star or black hole in core-collapse supernova (SN) explosions akin to SN 1998bw (e.g., DDD2002; Dar & De Rújula 2004; DDD2009a and references therein). Both, the prompt pulses and early-time X-ray flares are produced by the thermal electrons in the CBs by inverse Compton scattering (ICS) of photons emitted/scattered into a cavity created by the wind/ejecta blown from the progenitor star long before the GRB. The prompt keV-MeV pulses in long GRBs are produced by CBs ejected in the early episodes of mass accretion. As the accretion material is consumed, one may expect the engine’s activity to weaken. X-ray flares during the decay of the prompt emission and the early afterglow phase are produced in such delayed episodes of mass accretion, which result in ejections of CBs with smaller Lorentz factors.

In the CB model, the lightcurve of ICS pulses/flares is given approximately by (DDD2009a):

$$E \frac{d^2 N_\gamma}{dt dE}(E, t) \approx A \frac{t^2 / \Delta t^2}{(1 + t^2 / \Delta t^2)^2} E^{-\beta_g} e^{-E/E_p(t)}, \quad (1)$$

where $t = T - T_i$ with T being the time after trigger and T_i the beginning time of the pulse/flare after trigger. A is a constant which depends on the CB’s baryon number, Lorentz

and Doppler factors, on the density of the glory light and on the redshift and distance of the GRB. For $\beta_g=0$ (thin thermal spectrum of the glory photons), $E_p(t)$ is the peak energy of $E d^2 N_\gamma/dE dt$ at time t . Thus, in the CB model, each ICS pulse/flare in the GRB lightcurve is described by four parameters, A , $\Delta t(E)$, $E_p(t)$ and the beginning time of the pulse T_i when t is taken to be 0.

The temporal behaviour of $E_p(t)$ depends on the self-absorption properties of the CBs and the spatial distribution of the seed photons in the glory which are not well known. Roughly, the peak energy $E_p(t)$ is given by (DDD2009a):

$$E_p(t) \approx E_p(0) \frac{t_p^k}{t^k + t_p^k}, \quad (2)$$

with t_p being the time (after the beginning of the flare) when the ICS photon count rate reaches its peak value and $2 \lesssim k \lesssim 3$ in order to accommodate the observed time dependence of E_p at late time in several single-pulse GRBs. For $E \ll E_p$, $E_p(t_p) = E_p$, where E_p is the peak energy of the time-integrated spectrum of the ICS pulse/flare (DDD2009a).

If absorption in the CB is dominated by free-free transitions then roughly, $\Delta t(E) \propto E^{-0.5}$, and for $E \ll E_p$ the lightcurve of an ICF is approximately a function of $E t^2$ (the ‘ $E t^2$ law’), with a peak at $t = \Delta t$, a full width at half maximum, $\text{FWHM} \approx 2 \Delta t$ and a rise time from half peak value to peak value, $\text{RT} \approx 0.30 \text{FWHM}$ independent of E . Note that the approximate $E t^2$ law makes the late decline sensitive only to the product $E_p t_p^2$ and not to their individual values.

The evolution of the effective photon spectral index $\Gamma(t) = 1 + \beta$ of *isolated* ICS pulses/flares is given approximately (DDD2008) by,

$$\Gamma(t) \approx 1 + \frac{d \log(F_\nu)}{d(\log E)} \approx 1 + \beta_g + \frac{E(t^2 + t_p^2)}{E_p(0) t_p^2} \sim a + b t^2. \quad (3)$$

The $\sim t^2$ rise of Γ during the fast decline phase of an ICS pulse/flare stops when a second pulse/flare or the power-law tail of SR flare (DDD2009a) that follows the ICS pulse/flare begins to dominate F_ν (DDD2008). Because of the exponential decay of the ICS pulses/flares, when the SR emission takes over the photon spectral index drops sharply to its constant typical SR value $\Gamma_X \sim 2.1$ (DDD2002).

2.2. SR flares

Synchrotron radiation begins when the jet of CBs crosses the wind/ejecta which was blown from the progenitor star long before the GRB and continues during its deceleration

in the interstellar medium. During these phases the electrons of the ionized gas in front of the CBs, which are swept in and Fermi-accelerated by the CBs turbulent magnetic fields, emit synchrotron radiation (SR) that dominates the prompt optical flares (DDD2009a; Dado & Dar 2009a,b) and the following broad band afterglow emission. ICS of the SR radiation by the same electrons dominates the ‘prompt’ high energy (GeV) emission that takes place simultaneously with the ‘prompt’ optical emission (Dado & Dar 2009b). Assuming a canonical density profile of the wind/ejecta, $n(r) \propto \Theta(r-r_w) e^{-2l/(r-r_w)}/(r-r_w)^2$, where r_w is the internal radius of the wind/ejecta, $r-r_w=l$ at max n and Θ is a step function equal to zero for negative argument and to 1 for positive argument, the early time SR flares (SRFs) have the lightcurve shape (DDD2009a, Dado & Dar 2009a):

$$F_\nu[t] \propto \frac{e^{-a_w/t} t^{1-\beta}}{t^2 + t_{exp}^2} \nu^{-\beta} \rightarrow t^{-(1+\beta)} \nu^{-\beta}, \quad (4)$$

where $t=T-T_w$, T is the observer time after trigger and T_w is the observer time when the CB reach the wind/ejecta at r_w . Such a lightcurve has a flare like shape, i.e., a fast rise followed by a power-law decay. Since the X-ray band is well above the ‘bend’ frequency (DDD2009a), the X-ray flare has a temporal decay index $1+\beta_X \approx 1+p/2 \sim 2.1$ where p is the injection spectral index of the Fermi accelerated electrons (DDD2002). The beginning of the ‘prompt’ keV-MeV synchrotron emission that follows the ICS pulse/flare is usually hidden under it. But, because of the exponential decay of the ICS pulse/flare, the tail of the SR flare, which decays like $F_\nu \propto t^{-1} \nu^{-(1+\beta)}$, takes over and becomes visible in many GRBs (DDD2009a).

Long GRBs are mostly produced in core collapse supernova explosions (DDD2009a and references therein) which usually take place in star formation regions (SFRs). In that case Eq. (4) describes also the late-time SRF which is produced when the jet crosses the boundary of the SFR into the ISM or the halo of the host galaxy. This usually takes place around $t \approx (1+z) R_{SFR}/2c\gamma^2$ which for typical parameters of long GRBs happens between 10^4 and 10^5 sec.

3. Slowly rising late-time afterglows of XRFs

In the CB model, ordinary GRBs are observed mostly from viewing angles $\theta \sim 1/\gamma$ relative to the CBs’ direction of motion. X-ray flashes (XRFs) are ordinary GRBs observed from much larger viewing angles, $\theta > 3/\gamma$ and then $\delta < \gamma/5$ (Dar & De Rujula 2000; DDD2004). Such small Doppler factors of XRFs compared to $\delta \sim \gamma$ in ordinary GRBs, yield $E_{iso} \propto \delta^3$ smaller by roughly two orders of magnitude, $(1+z) E_p \propto \delta$ smaller by roughly a factor $< 1/5$, and lightcurves in the observer frame that are stretched in time by a factor $\gamma/\delta > 5$, compared to their respective values in ordinary GRBs. The unabsorbed spectral

energy density of their emitted SR is given by (DDD2009a and references therein),

$$F_\nu[t] \propto \gamma(t)^{3\beta-1} \delta(t)^{3+\beta} \nu^{-\beta}, \quad (5)$$

where $\beta_X \approx 1.1$ and $\beta_{opt}(t=0) \sim 0.5$. Relativistic energy-momentum conservation yields the deceleration-law of CBs of a baryon number N_B and a radius R in an ISM with a constant density n (DDD2009a and references therein):

$$\gamma(t) = \frac{\gamma_0}{[\sqrt{(1 + \theta^2 \gamma_0^2)^2 + t/t_0} - \theta^2 \gamma_0^2]^{1/2}}, \quad (6)$$

with $t_0 = (1+z) N_B / 8 c n \pi R^2 \gamma_0^3$. Thus, the shape of the entire lightcurve of the SR afterglow, after entering the constant-density ISM, depends only on three parameters, the product $\gamma_0 \theta$, the deceleration time scale t_0 and the spectral index β .

Since $\gamma(t)$ decreases with time, it follows from Eq. (5) has a maximum when $\gamma(t) \theta = [(4\beta+2)/(4-2\beta)]^{1/2}$. If the CB enters the constant-density ISM with a larger initial value of $\gamma(t) \theta$, then $F_\nu[t]$ increases slowly as function of time until $\gamma(t) \theta$ has decreased to this value. In the X-ray band $\beta_X \approx 1.1$ and the peak value of $F_\nu[t]$ is reached when $\gamma(t) \theta$ decreased to 1.89. In the optical band, initially $\beta_{opt}=0.5$ and the peak value of $F_\nu[t]$ is reached when $\gamma(t) \theta$ decreased to 1.21. Thus after their prompt emission phase, XRFs whose $\gamma(0) \theta > 3$ exhibit a slowly rising AG if the progenitor's wind/ejecta has not slowed down the CBs such that $\gamma(t) \theta$ crossed below the above peak values upon entering the constant density ISM.

Note that slowly rising X-ray and optical afterglows are not limited to XRFs. They can be found also in relatively 'soft' GRBs with $1.89 < \gamma(0) \theta < 3$. GRBs 091029 and 091127 whose lightcurves are shown in Figs. 7,8,9 may be such cases.

As can be seen from Eq. (6), γ and δ in a constant density ISM change little as long as $t \ll t_b = [1 + \gamma_0^2 \theta^2]^2 t_0$ and Eq. (5) yields the 'plateau' or shallow decay phase of canonical AGs. For $t \gg t_b$, γ and δ decrease like $t^{-1/4}$ and the AG has an asymptotic power-law decay,

$$F_\nu[t] \propto t^{-\beta-1/2} \nu^{-\beta}. \quad (7)$$

The transition $\gamma_0 \rightarrow \gamma_0 (t/t_0)^{-1/4}$ around t_b induces a bend in the AG, the so called 'jet break'. The post break power-law decline of the AG (Eq. 7) is independent of the values of $\gamma_0 \theta$ and t_0 . Because of the relatively small value of γ at late time, the X-ray and optical bands are both well above the bend frequency and then $\beta_O \approx \beta_X \approx 1.1$, yielding the same asymptotic decline, $F_\nu[t] \sim t^{-1.6} \nu^{-1.1}$, in both the X-ray and optical bands.

4. Comparison with observations

In Fig. 1 we compare the measured equivalent isotropic energy $E_{iso} = (1.1 \pm 0.1) \times 10^{53}$ erg and the rest frame peak energy $(1+z) E_p = 222_{-36}^{+81}$ keV of GRB081028, and those of other ordinary GRBs and XRFs with known redshift. The $[E_p, E_{iso}]$ correlations predicted by the CB model (DDD2007 and references therein) for LGRBs and SHBs are indicated by the thick lines. As can be seen, the measured values of E_{iso} and E_p in GRB081028 are normal for ordinary GRBs and satisfy the predicted CB model correlation, while XRFs which are GRBs with small E_p have much smaller values of E_{iso} than those of ordinary GRBs. We have also indicated in Fig. 1 their values for a recently measured ‘soft’ GRB 091127.

In Fig. 2 we compare the Swift BAT 15-150 keV lightcurve of GRB081028 (Margutti et al. 2009) and its CB model description in terms of 2 prompt ICS pulses, each one described by Eq. (1) with $E_p(t)$ as given by Eq. (2) with $E_p(t_p) = E_p$ and the E_p values reported by Margutti et al. 2009. In order to minimize the number of adjustable parameters in the CB model description we have assumed $\beta_g = 0$, which results in a simple cut-off power-law behaviour of the spectrum of the ICS pulses/flares with a cutoff energy equal to E_p (see Eq. (1)). The normalization constant A , the beginning time T_i and the width $\Delta(E)$ at the BAT mid-band energy $E = 82.5$ keV, and the peak energy $E_p = E_p(t_p)$ of each pulse, which were used in the CB model description of the lightcurve, are listed in Table 1.

In Fig. 3 we compare the 0.3-10 keV lightcurve of GRB081028 reported in the Swift/XRT light curve repository (http://www.swift.ac.uk/xrt_curves/, Evans et al. 2009) and its CB model description as a sum of 3 early-time ICS flares (ICFs) as given by Eq. (1) and a late-time synchrotron radiation flare (SRF) as given by Eq. (4). In order to minimize the number of parameters, we assumed that after their prompt emission, the deceleration of the two leading CBs and their expansion merged them into a single leading plasmoid (CB). The best fit parameters used in the CB model description are listed in Table 1. The CB description of the lightcurve during the orbital gap in the Swift XRT data between 850 and 4130 sec is highly uncertain and we have plotted only the rise and tail of the third ICF. The entire CB model lightcurve has $\chi^2/dof = 1.31$ for $dof = 499$. Note in particular that the power-law index of the late-time decay of the SR flare satisfies well the CB model relation $\alpha_X = \beta_X + 1 = \Gamma_X$ with $\Gamma_X = 2.091 (+0.063, -0.060)$ that was reported in the Swift XRT lightcurve repository (Evans et al. 2009).

In Fig. 4 we compare the evolution of E_p during the fast decay of the prompt emission in GRB081028 and its CB model description as given by Eq. (2) with $k=3$. The value of k in individual pulses may actually be ~ 2 . The value $k=3$ is probably an effective value for the sum of ICS flares whose E_p values decrease rapidly with time as the activity of the central engine weakens and produces smaller Lorentz factors.

In Fig. 5 we compare the effective photon spectral index that was inferred by Margutti et al. (2009) from the XRT data on GRB081028 in the 0.3-10 keV energy range and that inferred from the CB model description, Eq. (3), at mid energy $E=5.15$ keV. Due to the orbital gap in the Swift XRT data, the predicted photon spectral index between 850 and 4130 sec is highly uncertain.

In Fig. 6 we compare the 0.3-10 keV X-ray lightcurve of XRF080707 which was measured with the Swift/XRT and its CB model description in terms of a tail of an ICS flare and a rising late-time afterglow of a GRB viewed far off axis. The parameters of the CB model description are listed in table 2.

In Fig. 7 we compare the 0.3-10 keV X-ray lightcurve of the soft GRB091029 which was measured with the Swift/XRT and its CB model description in terms of a tail of two ICS flares, a rising late-time afterglow of a GRB viewed far off axis and a late time SR flare presumably produced during its passage through the boundary of the star formation region into the ISM or the halo of the host galaxy. The parameters of the CB model description are listed in table 2.

In Fig. 8 we compare the 0.3-10 keV X-ray lightcurve of the soft GRB091127 ($(1+z) E_p = 54 \pm 3$ keV; Wilson et al. GCN 10204) that was measured with the Swift XRT (XRT light curve repository, Evans et al. 2009) and its CB model description in terms of a slowly rising afterglow of a ‘soft’ GRB . The parameters of the CB model description are listed in table 2.

In Fig. 9 we compare the lightcurve of the R band afterglow of the ‘soft’ GRB 091127 as reported in recent GCNs (Smith et al. 10192; Updike et al. 10195; Xu et al. 10196,10205; Klotz et al. 10200,10208; Andreev et al. 10207; Haislip et al. 10219, 10230, 10249; Kinugasa et al. 10248) and its CB model description in terms of an early flare overtaken by a slowly rising afterglow of a ‘soft’ GRB with a superimposed light from a supernova akin to SN1998bw placed at the burst location. The prompt emission flare is not constraint by the single data point. The data and the CB model predictions were not corrected for extinction in our Galaxy and in the host galaxy.

5. Summary and conclusions

In the CB model, most XRF and soft GRBs are ordinary GRBs observed from a far off-axis viewing angle, i.e, viewing angles much larger than those of typical GRBs. This implies smaller value of $(1+z) E_p$, much smaller value of E_{iso} , prompt pulses, flares and afterglows much more stretched in time, and a slowly rising late-time afterglow, which turns

into an asymptotic power-law decay $\sim t^{-\Gamma+1/2}$, as demonstrated here for XRF080707 and the soft GRBs 091029 and 091127.

GRB081028 was observed from space with the BAT and XRT aboard Swift and from the ground with optical telescopes. The observations provided detailed information on its properties, which differ from those expected from a far off-axis GRB. The equivalent isotropic energy E_{iso} and peak energy $(1+z) E_p$ of its prompt emission are typical of ordinary GRBs and satisfy the $[(1+z)E_p, E_{iso}]$ correlation for ordinary GRBs (Fig. 1): The measured value of E_{iso} yields $(1+z) E_p \sim 280$ keV, in good agreement with its measured value $(1+z) E_p = 222_{-36}^{+81}$ keV, which is much larger than the typical values of E_p in XRFs. Its lightcurves are well described by the CB model assuming an ordinary GRB: The BAT 15-150 keV lightcurve of the prompt emission is well described by a sum of two pulses/flares produced by two CBs by ICS of glory photons (Fig. 2). Its 0.3-10 keV X-ray lightcurve, which begins during the second peak, shows a steep decay of the prompt emission accompanied by a rapid spectral softening with flares superimposed. It is well described by a sum of three X-ray flares produced by ICS of glory photons by the electrons in CBs late ejected by a weakening central engine (Fig. 3). The smoothly rising X-ray AG, which follows the steep decay, peaks around 22 ks, after which it turns into a power-law decay. This behaviour of the AG is well described by a late-time SRF (Fig. 3). In particular, the photon spectral index during the late time flare remains constant, $\Gamma_X = 2.04 \pm 0.06$, as expected in the CB model for SRFs. Moreover, the power-law decay of the SRF has an index $\alpha = 2.09$ which satisfies within errors the CB model prediction (DDD2009a) $\alpha_X = \beta_X + 1 = \Gamma = 2.091 \pm 0.063$, Had it been an ordinary synchrotron AG of a far-off axis GRB, i.e., like that of XRFs, its temporal index would have been $\alpha_X = \beta_X + 1/2 = \Gamma - 1/2 \approx 1.6$ (DDD2009a), independent of viewing angle, in contradiction with the observed value, $\alpha \sim 2.1$. These temporal and spectral properties of the late-time flare in the AG of GRB081028 and the normal values of E_{iso} and E_p of its prompt emission agree well with the CB model interpretation of the re-brightening of its afterglow - i.e., a late-time SR flare produced by the same jet that produced GRB081028, presumably during its passage through the boundary of the star formation region where GRB081028 took place, into the ISM or the halo of the host galaxy.

Acknowledgment The authors are grateful to Raffaella Margutti for kindly providing the tabulated data used in Figs. 1,3,4.

REFERENCES

- Chiang, J. & Dermer, C. D. 1997, arXiv:9708035
 Dado, S., Dar, A. 2009a, arXiv:0908.0650

- Dado, S., Dar, A. 2009b, arXiv:0910.0687
- Dado, S., Dar, A. & De Rújula, A. 2002, *A&A*, 388, 1079 (DDD2002)
- Dado, S., Dar, A. & De Rújula, A. 2004, *A&A*, 422, 381 (DDD2004)
- Dado, S., Dar, A. & De Rújula, A. 2007, *ApJ*, 663, 400 (DDD2007)
- Dado, S., Dar, A. & De Rújula, A. 2008, *ApJ*, 681, 1408 (DDD2008)
- Dado, S., Dar, A. & De Rújula, A. 2009a, *ApJ*, 696, 994 (DDD2009a)
- Dado, S., Dar, A. & De Rújula, A. 2009b, *ApJ*, 693, 311 (DDD2009b)
- Dar, A. 1998, *ApJ*, 500, L93
- Dar, A. & De Rújula, A. 2000, arXiv:astro-ph/0008474
- Dar, A. & De Rújula, A. 2004, *Phys. Rep.* 405, 203
- Evans, P., et al. 2007, *A&A*, 469, 379.
- Evans et al. 2009, *MNRAS*, submitted (arXiv:0812.3662)
- Galama, T. J., et al. 1998, *ApJ*, 497, L13
- Mangano, V. et al., 2007 *A&A*, 470, 105
- Margutti, R. et al. 2009, arXiv:0910.3166
- Piro, L., et al. 1998, *A&A*, 331, L4
- Shaviv, N. & Dar, A. 1995, *ApJ*, 447, 863

Table 1. The parameters of the early-time ICS and late-time SR flares used in the CB model descriptions of the Swift/BAT and XRT lightcurves of GRB081028.

flare	T_i [s]	Δt [s]	E_p [keV]
BAT ICF1	20.26	73.12	50
BAT ICF2	144.0	78.10	65
XRT ICF1	205.5	134.6	5.14
XRT ICF2	411.2	235	0.19
XRT ICF3	665.2	—	0.14
	T_w [s]	t_{exp} [s]	a_w [s]
XRT SRF	7038	21176	7056

Table 2. The parameters of the early-time ICS and late-time SR afterglow and flares used in the CB model descriptions of the X-ray lightcurves of XRFs 080707 and 091029.

flare	T_i [s]	Δt [s]	E_p [keV]
XRF080707 ICF1	4.18	31.3	9.0
GRB091029 ICF1	~ 0	38.8	9.8
GRB091029 ICF2	218.5	102.5	10.93
	T_w [s]	t_{exp} [s]	a_w [s]
GRB091029 SRF	2.09×10^5	2.46×10^5	9.8×10^4
	$\gamma(0)\theta$	t_b	Γ_X
XRF080707 AG	3.85	2111	2.06
GRB091029 AG	2.35	5754	2.01
GRB091127 AG	2.42	1365	2.03

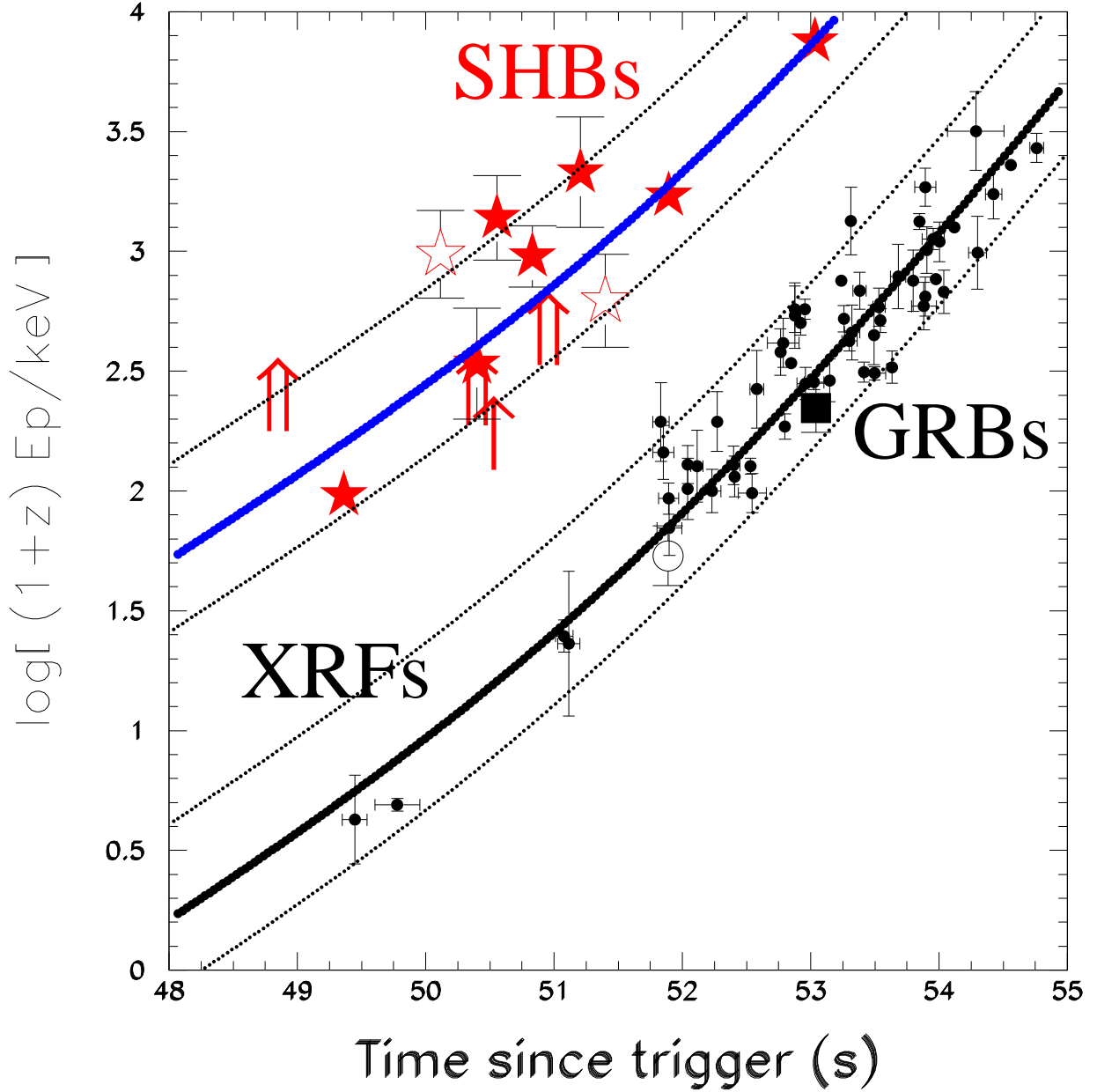


Fig. 1.— Comparison between the observed correlation $[E_p, E_{iso}]$ in GRBs and the correlation predicted by the CB model (thick lines) in LGRBs/XRFs (DDD2007, Eq.(4)) and in SHBs (DDD2009b, Eq.(22)) with known redshift. The long GRB081028 is indicated by a full black square.

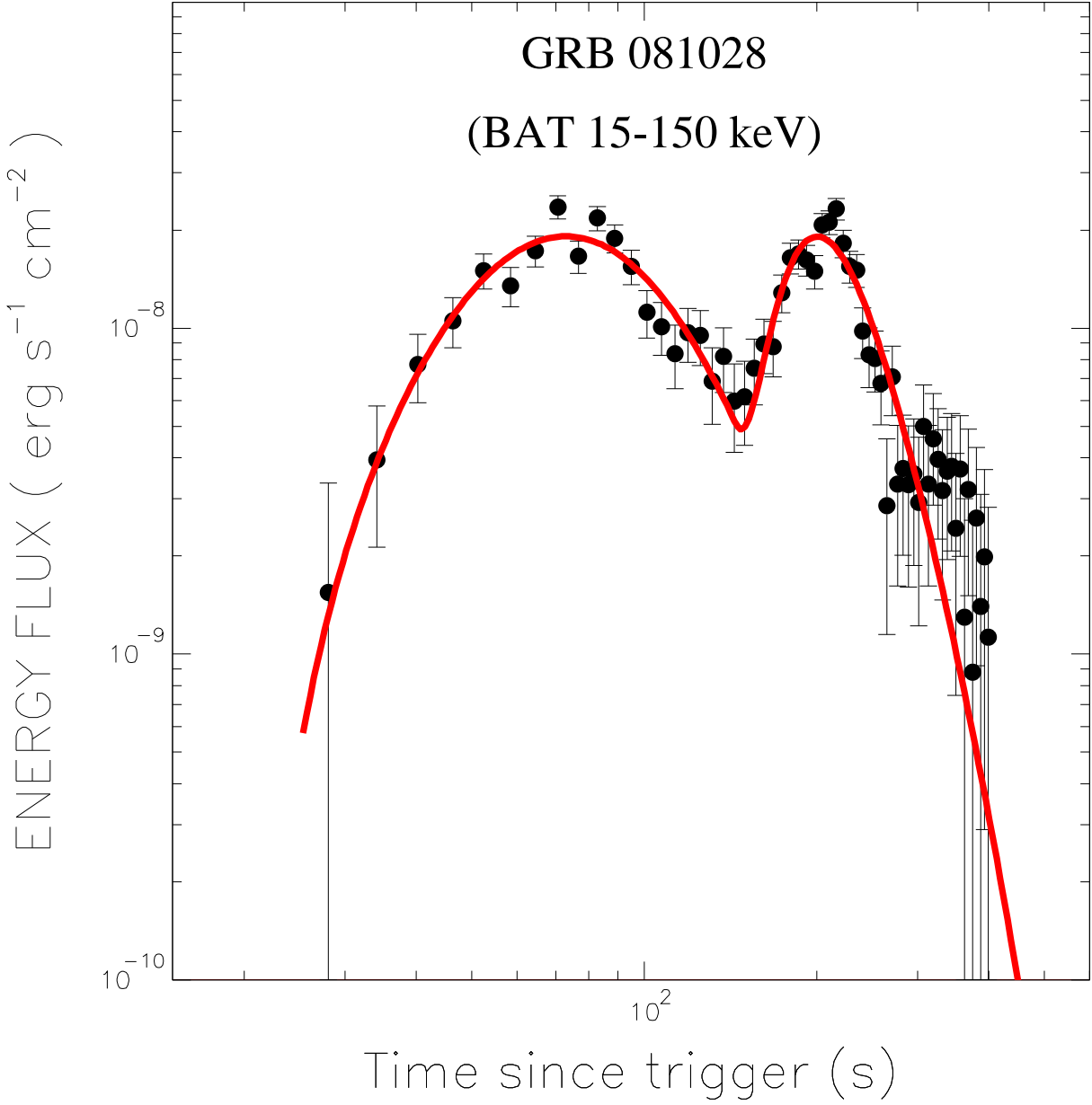


Fig. 2.— Comparison between the Swift BAT lightcurve of the prompt 15-150 keV emission in GRB081028 (Margutti et al. 2009) and its CB model description in terms of two ICS flares (see the text for details).

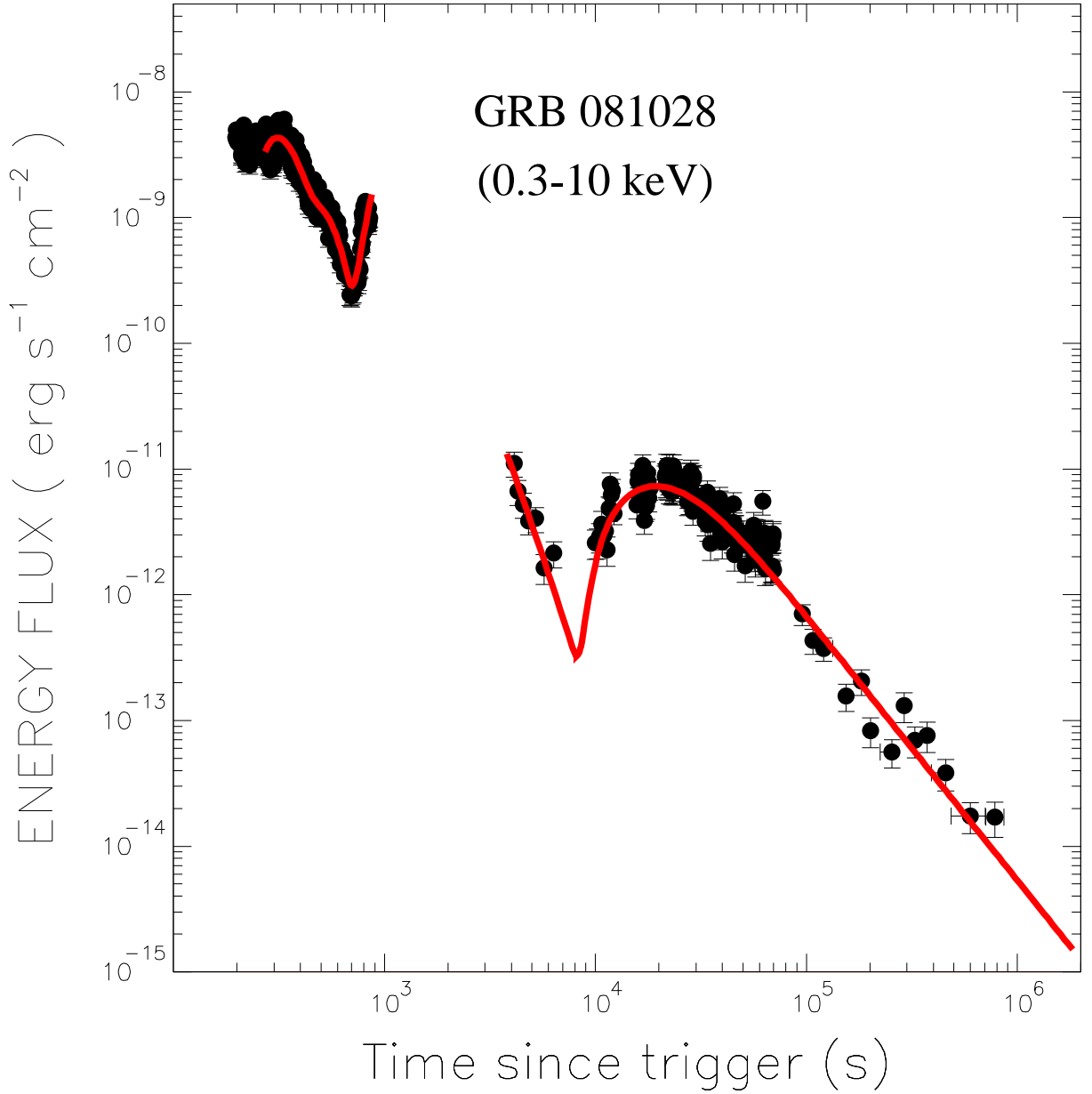


Fig. 3.— Comparison between the Swift XRT 0.3-10 keV X-ray lightcurve of GRB081028 (XRT lightcurve repository, Evans et al. 2009) and its CB model description in terms of 3 early-time ICS flares and a late-time SR flare and the parameters listed in table (see the text for details).

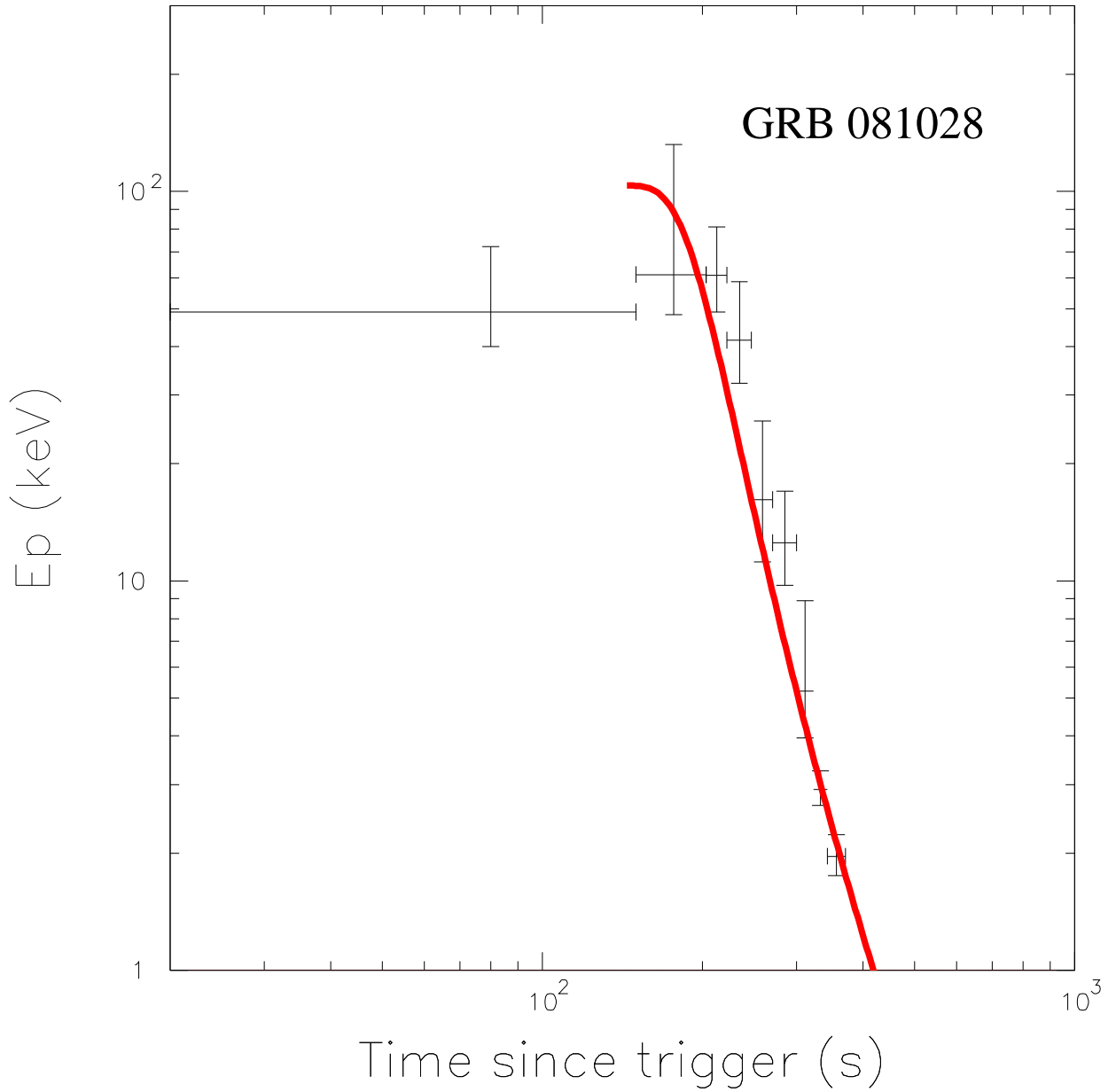


Fig. 4.— Comparison between the temporal variation of the peak energy $E_p(t)$ in GRB081028 during the fast decay phase of the prompt emission that was inferred by Margutti et al. (2009) from the Swift BAT and XRT observations, and its CB model description (see text for details).

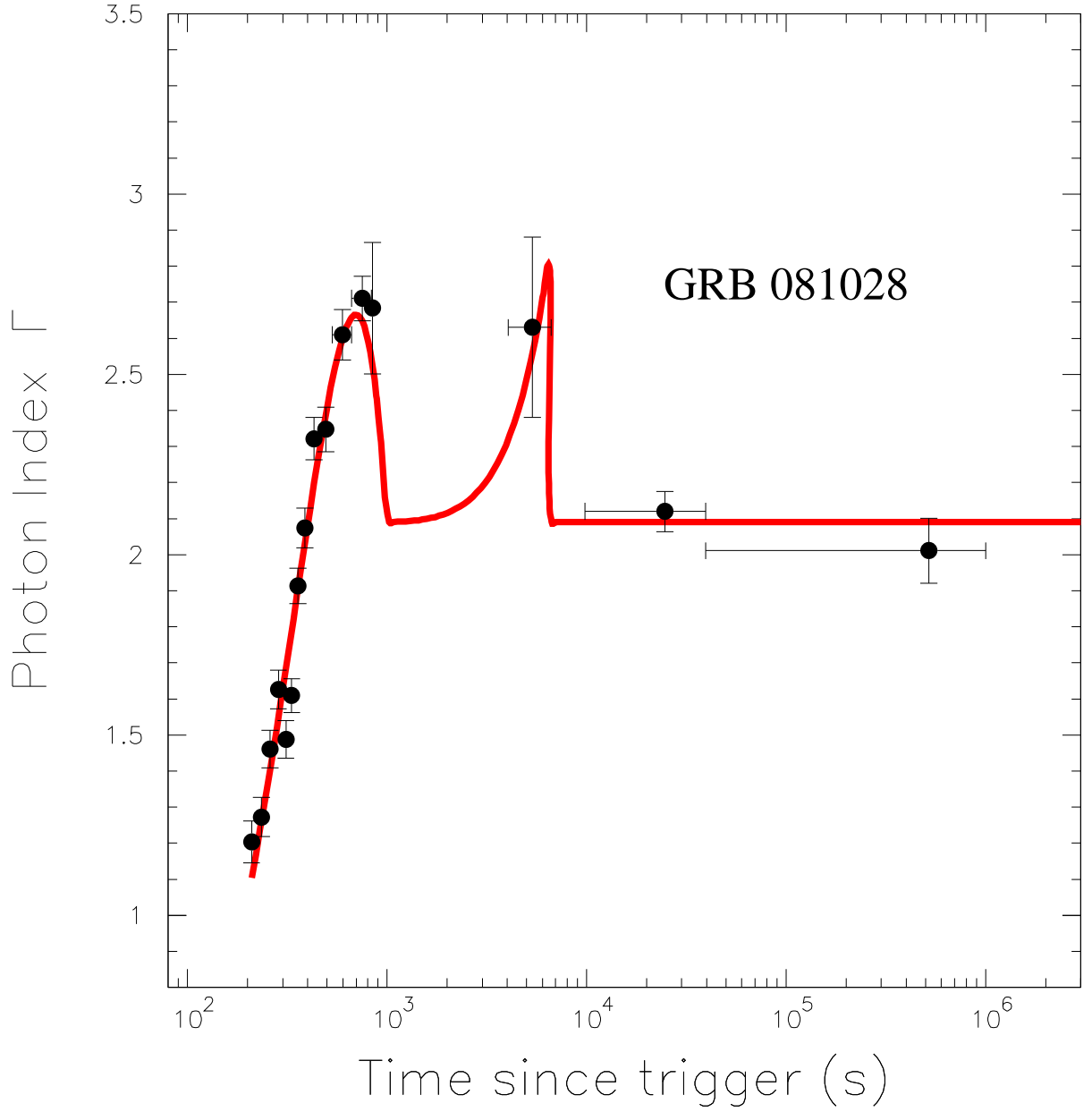


Fig. 5.— Comparison between the effective photon spectral index of the 0.3-10 keV lightcurve of GRB081028, which was inferred by Margutti et al. (2009) from the Swift XRT observations, and that which follows from the CB model description of the XRT lightcurve (see the text for details).

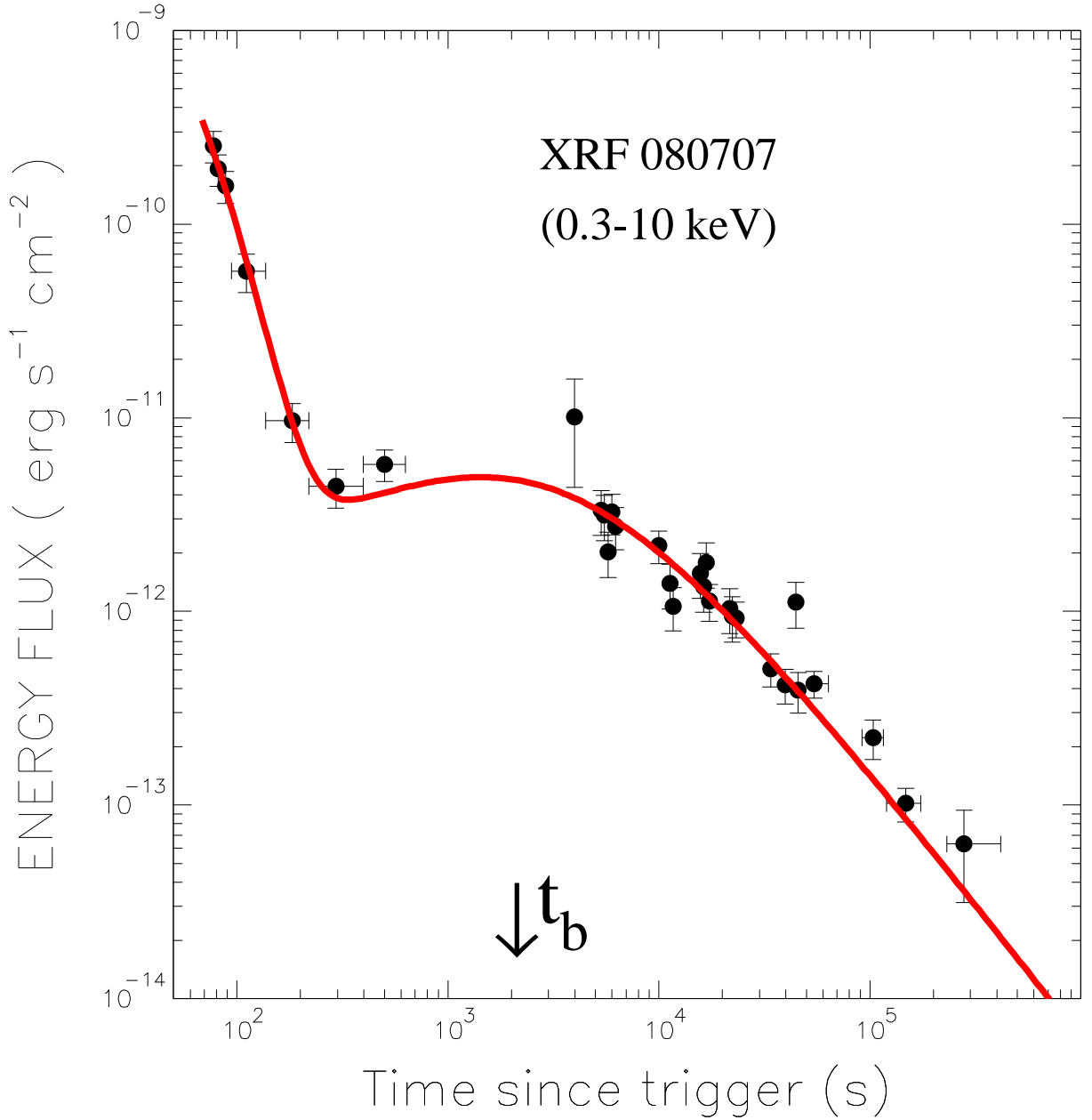


Fig. 6.— Comparison between the 0.3-10 keV X-ray lightcurve of GRB081028 reported in the Swift/XRT lightcurve repository http://www.swift.ac.uk/xrt_curves/, Evans et al. 2009) and its CB model description in terms of the tail of an early-time ICS flare and a late-time afterglow assuming a constant density ISM. The parameters that were used are listed in Table 2. (see the text for details).

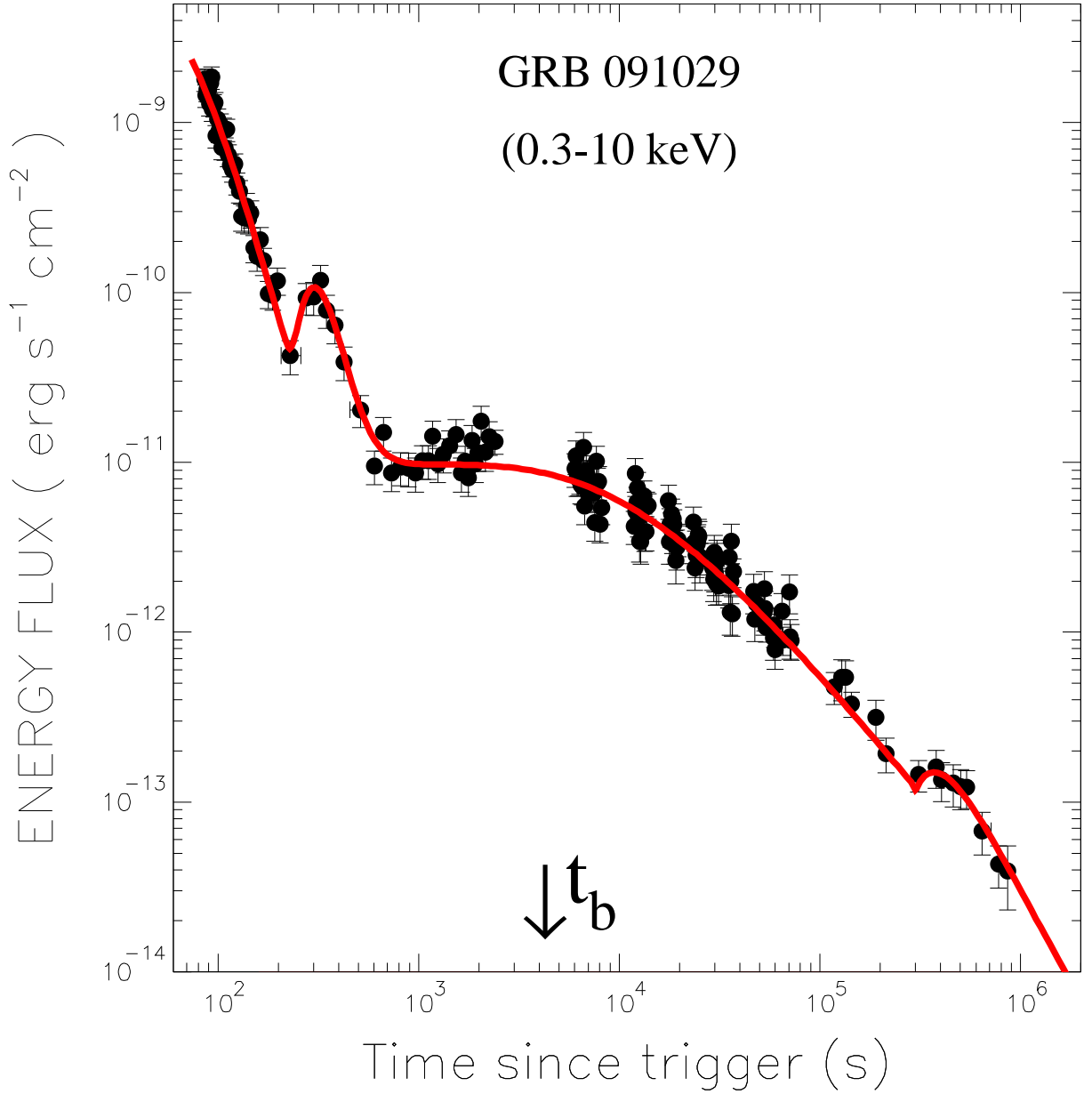


Fig. 7.— Comparison between the Swift XRT 0.3-10 keV X-ray lightcurve of XRF 091029 (XRT lightcurve repository, Evans et al. 2009) and its CB model description in terms of two early-time ICS flare, a late-time afterglow assuming a constant density ISM and a late time SR flare. The parameters that were used are listed in Table 2. (see the text for details).

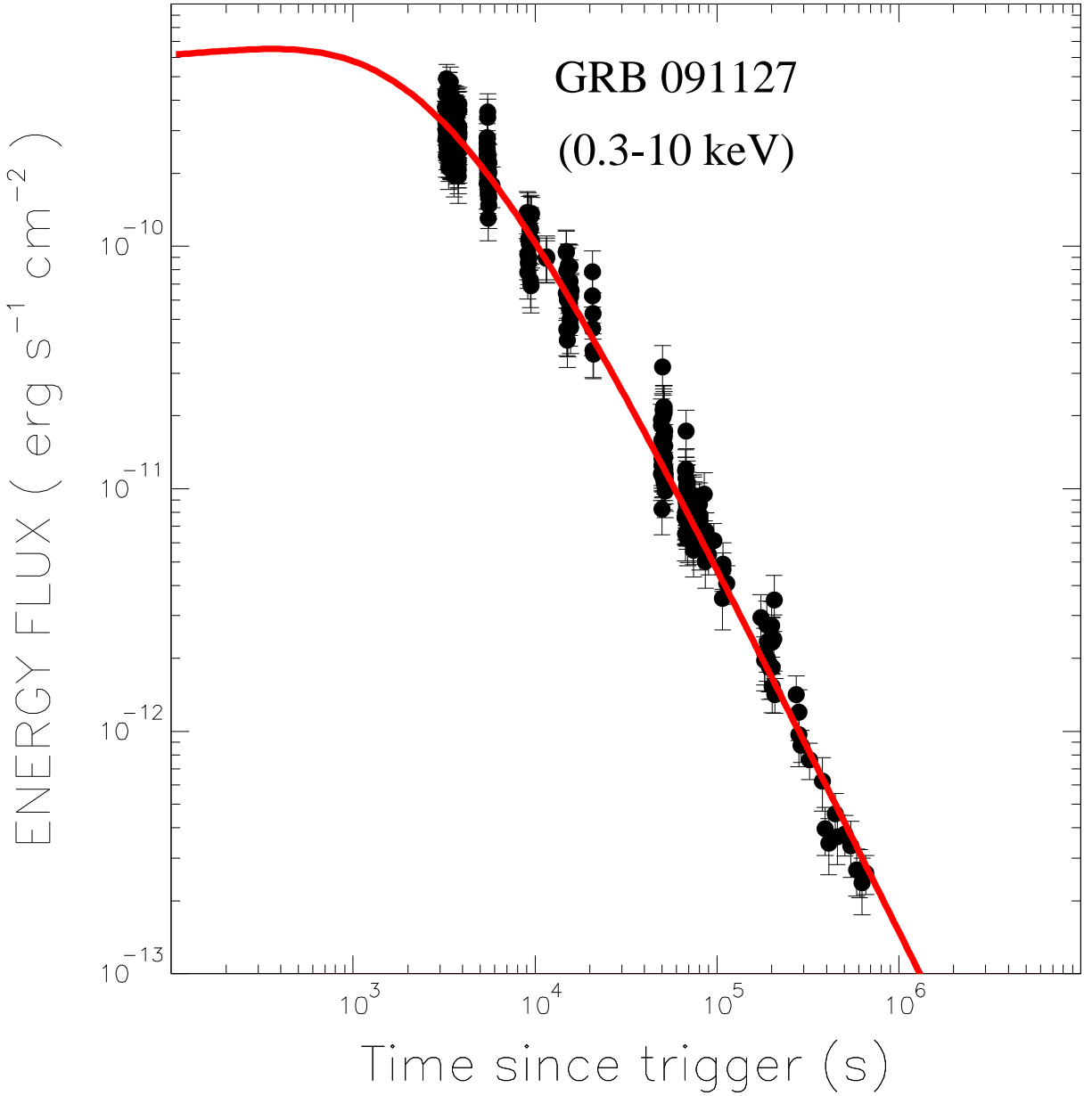


Fig. 8.— Comparison between the 0.3-10 keV X-ray lightcurve of the soft GRB091127 reported in the Swift/XRT lightcurve repository (Evans et al. 2009) and its CB model description in terms of a rising late-time afterglow. The parameters that were used are listed in Table 2. (see the text for details).

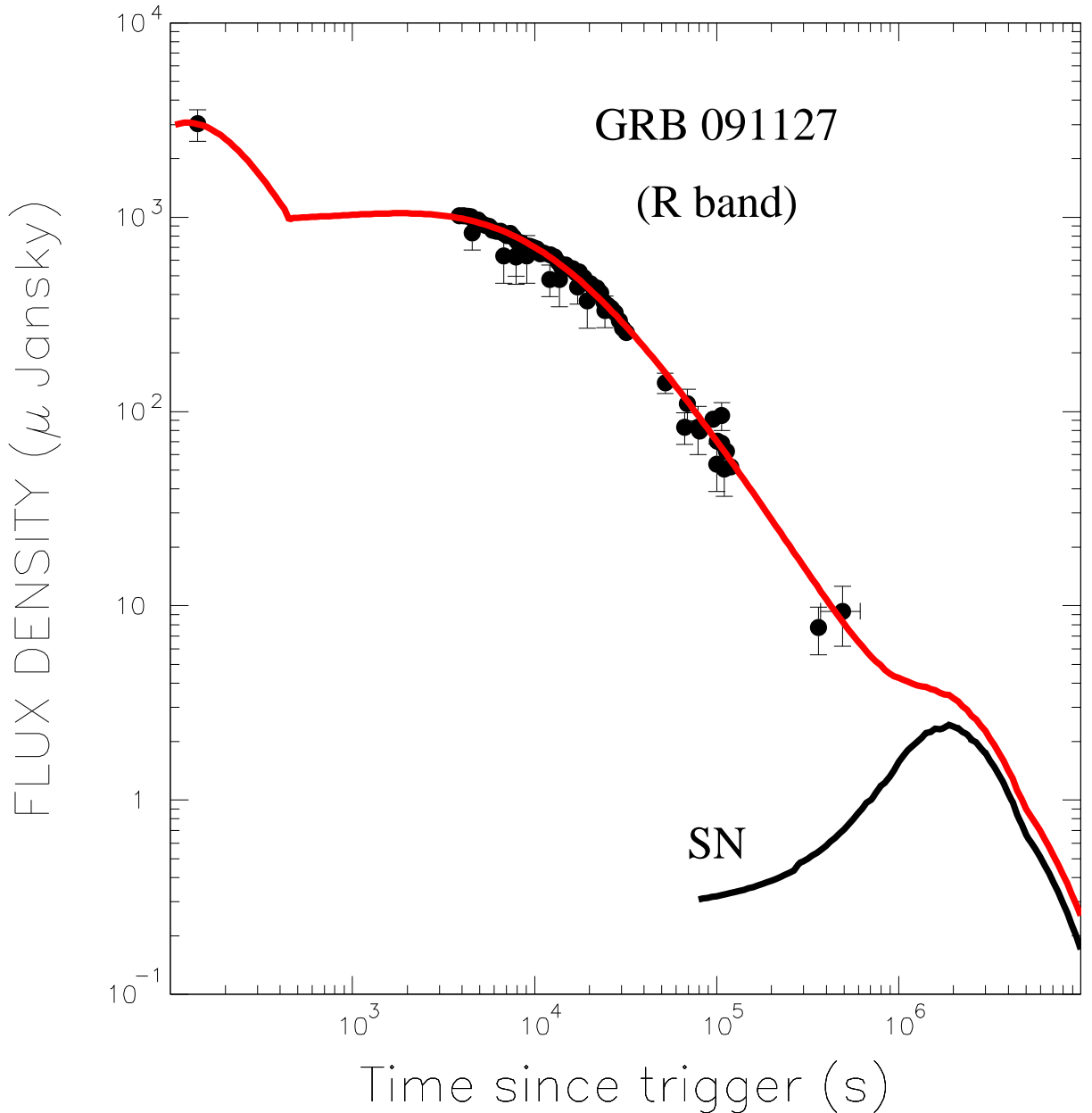


Fig. 9.— Comparison between the R band light curve of the soft GRB 091127 as reported in recent GCNs (Smith et al. 10192; Updike et al. 10195; Xu et al. 10196,10205; Klotz et al. 10200,10208; Andreev et al. 10207; Haislip et al. 10219, 10230, 10249; Kinugasa et al. 10248) and its CB model description in terms of a prompt optical flare from the jet collision with the progenitor’s wind/ejecta prior to the GRB, a slowly rising AG with a superimposed light from an SN akin to SN1998bw at the GRB location. The parameters $\gamma(0)\theta$, and the late time value of Γ of the rising AG are those obtained from the CB model description of the X-ray lightcurve (see the text for details).